

# Dose-Response Relationships for *N*7-(2-Hydroxyethyl)Guanine Induced by Low-Dose [<sup>14</sup>C]Ethylene Oxide: Evidence for a Novel Mechanism of Endogenous Adduct Formation

Debbie A. Marsden,<sup>1</sup> Donald J.L. Jones,<sup>1</sup> Robert G. Britton,<sup>1</sup> Ted Ognibene,<sup>2</sup> Esther Ubick,<sup>2</sup> George E. Johnson,<sup>3</sup> Peter B. Farmer,<sup>1</sup> and Karen Brown<sup>1</sup>

<sup>1</sup>Department of Cancer Studies and Molecular Medicine, University of Leicester, Leicester, United Kingdom; <sup>2</sup>Lawrence Livermore National Laboratory, Livermore, California; and <sup>3</sup>Swansea University, Swansea, United Kingdom

## Abstract

Ethylene oxide (EO) is widely used in the chemical industry and is also formed in humans through the metabolic oxidation of ethylene, generated during physiologic processes. EO is classified as a human carcinogen and is a direct acting alkylating agent, primarily forming *N*7-(2-hydroxyethyl)guanine (*N*7-HEG). To conduct accurate human risk assessments, it is vital to ascertain the relative contribution of endogenously versus exogenously derived DNA damage and identify the sources of background lesions. We have therefore defined *in vivo* dose-response relationships over a concentration range relevant to human EO exposures using a dual-isotope approach. By combining liquid chromatography-tandem mass spectrometry and high-performance liquid chromatography-accelerator mass spectrometry analysis, both the endogenous and exogenous *N*7-HEG adducts were quantified in tissues of [<sup>14</sup>C]EO-treated rats. Levels of [<sup>14</sup>C]*N*7-HEG induced in spleen, liver, and stomach DNA increased in a linear manner from 0.002 to 4 adducts/10<sup>8</sup> nucleotides. More importantly, the extent of damage arising through this route was insignificant compared with the background abundance of *N*7-HEG naturally present. However, at the two highest doses, [<sup>14</sup>C]EO exposure caused a significant increase in endogenous *N*7-HEG formation in liver and spleen, suggesting that EO can induce physiologic pathways responsible for ethylene generation *in vivo* and thereby indirectly promote *N*7-HEG production. We present evidence for a novel mechanism of adduct formation to explain this phenomenon, involving oxidative stress and 1-aminocyclopropane-1-carboxylic acid as a potential biosynthetic precursor to ethylene in mammalian cells. Based on the proposed pathway, *N*7-HEG may have potential as a biomarker of cellular oxidative stress. [Cancer Res 2009;69(7):3052–9]

## Introduction

Ethylene oxide (EO) is a widely used industrial intermediate in the manufacture of chemicals and is used as an agricultural fumigant and sterilizing agent, particularly for medical equipment and heat-sensitive goods (1). It is estimated that in the U.S. health care sector, as many as 325,000 people are exposed directly or incidentally to EO in the workplace (2). Whereas initial epidemiology studies suggested links between an elevated risk of leukemia

and stomach cancer and occupational exposure to EO (3–5), many subsequent reports are inconclusive or contradictory about the ability of EO to induce specific cancers or increase cancer-related mortality (6–9). Despite the conflicting epidemiologic evidence, EO is classified by the IARC as carcinogenic to humans, primarily based on results from animal carcinogenicity studies, the fact that it is a direct alkylating agent that elevates mutation frequencies in rodent models, and evidence of chromosomal damage in peripheral blood lymphocytes of exposed workers (10).

The mutagenicity and carcinogenicity of EO is attributed to reaction with DNA, leading to the formation of multiple 2-hydroxyethyl adducts (11, 12). The most abundant product, *N*7-(2-hydroxyethyl)guanine (*N*7-HEG), readily depurinates, leaving abasic sites with miscoding potential (13, 14). Measurement of *N*7-HEG in animal or human cellular DNA can provide a valuable biomarker of total EO exposure at the target site, vital information for risk assessment purposes. A confounding factor in evaluating the risks associated with EO inhalation is the fact that ethylene is also generated *in vivo* during normal physiologic processes and can be converted to the epoxide by cytochrome *P*450 2E1 (15). Humans are therefore continually exposed to EO, as illustrated by detectable *N*7-HEG at levels of ~1 to 10/10<sup>7</sup> nucleotides in lymphocytes isolated from people not knowingly in contact with EO (16–18). Physiologic sources of ethylene are believed to include methionine oxidation, lipid peroxidation, and the metabolizing activity of intestinal bacteria (19–21); however, the mechanisms of formation in mammalian systems have not been defined in any of these cases and the origins of endogenous *N*7-HEG adducts have never been directly shown.

For genotoxic carcinogens such as EO, the current regulatory stance assumes that a linear relationship exists between exposure, the formation of DNA lesions, and subsequent conversion into mutations, although measurable increases in mutagenic events are only associated with relatively high doses (22, 23). Consequently, demonstration that a chemical is able to form DNA adducts at high exposures is often taken as sufficient evidence for carcinogenic potential at lower doses. However, nothing is actually known about the dose-response relationships for occupational or environmentally generated EO at the low concentrations humans are exposed to. Furthermore, this position fails to recognize that practical risk thresholds may be apparent for certain genotoxic agents where high levels of structurally identical endogenous adducts also exist (24).

To assess the true risk associated with inhaled EO, distinct from that presented by ubiquitous background DNA damage caused by endogenous EO, it is necessary to distinguish between the two types of lesions and ascertain the relative contribution of damage arising from the different sources. Sensitivity limitations and an inability to differentiate identical adducts formed by multiple

**Requests for reprints:** Karen Brown, Department of Cancer Studies and Molecular Medicine, University of Leicester, Leicester LE2 7LX, United Kingdom. Phone: 44-116-223-1851; Fax: 44-116-223-1855; E-mail: kb20@le.ac.uk.

©2009 American Association for Cancer Research.  
doi:10.1158/0008-5472.CAN-08-4233

routes using conventional analysis methods have made this difficult to achieve. Accelerator mass spectrometry (AMS), a technique traditionally used in the archaeological and geological sciences, allows for the extremely sensitive and accurate tracing of rare long-lived radioisotopes, such as  $^{14}\text{C}$ , in biological samples (25). It is one of the most sensitive methods available for DNA adduct quantification, capable of detecting as little as  $\sim 1$  to  $10$  adducts/ $10^{12}$  nucleotides. Exploiting the attomole sensitivity of AMS, we have defined the *in vivo* dosimetry for EO over a concentration range relevant to humans using a dual-isotope approach, combining liquid chromatography-tandem mass spectrometry (LC-MS/MS) and high-performance liquid chromatography (HPLC)-AMS analysis for the quantification of endogenous and exogenous N7-HEG adducts, respectively, in tissues of [ $^{14}\text{C}$ ]EO-exposed rats. Results suggested a new mechanism of endogenous ethylene production in mammalian cells, mediated by oxidative stress and stimulated by EO administration. Further investigations revealed 1-aminocyclopropane-1-carboxylic acid (ACC) as a potential biosynthetic precursor to ethylene and subsequent N7-HEG formation.

## Materials and Methods

**Chemicals.** [ $^{14}\text{C}$ ]EO (52 mCi/mmol) was purchased from GE Healthcare Bio-Sciences. Solvents were acquired from Fisher and all other chemicals were purchased from Sigma unless otherwise stated.

**Animals and treatment.** Male Fischer-344 rats (6–7 wk old) purchased from Harlan were randomized into groups and acclimatized for 7 d in standard cages. Dosing solutions were prepared by condensing  $^{14}\text{C}$ -labeled EO gas on ice and producing a stock solution by addition of ice-cold PBS (pH 7.0), which was then diluted as required. All solutions were prepared fresh on a daily basis using a new ampoule of [ $^{14}\text{C}$ ]EO and were kept on ice in sealed containers and then allowed to reach room temperature over  $\sim 10$  min immediately before dosing. Rats (four per group) were administered [ $^{14}\text{C}$ ]EO or vehicle only at doses of 0.1, 0.05, 0.01, 0.005, 0.001, 0.0005, 0.0001, or 0 mg/kg daily by i.p. injection for 3 consecutive days. Animals were sacrificed 4 h after the last dose. Blood was obtained by cardiac puncture after culling and specified tissues were removed. DNA was extracted using a Qiagen 500 tip kit (Qiagen, Inc.) according to the manufacturer's protocol. For the quantitation of adduct levels, samples from only three animals per group were used due to the costs associated with AMS analysis. For determination of tissue and blood concentrations of [ $^{14}\text{C}$ ]EO equivalents, samples were analyzed from all four rats.

**Liquid scintillation counting.** Liquid scintillation counting (LSC) was performed on a Beckman LS 6500 scintillation system (Beckman Coulter). Hydrofluor scintillation fluid (6 mL; National Diagnostics) was added to 40 mg of tissue or 100  $\mu\text{L}$  blood and samples were counted for 10 min. To allow direct comparisons between tissue and blood, values were expressed in terms of pg/mg on the basis that 1 mL blood has a mass of 1 g.

**Isolation of N7-HEG by neutral thermal depurination.** Typically, DNA samples (100  $\mu\text{g}$ , 1  $\mu\text{g}/\mu\text{L}$  in water) were added to 1,000 fmol of the [ $^{15}\text{N}_5$ ]N7-HEG internal standard and incubated at  $100^\circ\text{C}$  for 15 min. Ice-cold ethanol was added (80  $\mu\text{L}$ ) and the samples were centrifuged through a Microcon filter (3,000 molecular weight cutoff) at 14,000 rpm (1 h, room temperature). The filtrate was split in half, with one aliquot being used for HPLC-AMS analysis and the remainder concentrated and redissolved in 100  $\mu\text{L}$  of 40% methanol in 0.5% acetic acid for LC-MS/MS analysis. Both  $^{14}\text{C}$ -labeled and endogenous N7-HEG adduct levels were determined in three rats from each treatment group.

**Determination of N7-HEG in DNA samples by LC-MS/MS.** Unlabeled N7-HEG adducts were quantified using our validated LC-MS/MS method as described previously (26). Each sample of hydrolyzed DNA (50  $\mu\text{g}$ ) was injected onto a Zorbax 300SB  $\text{C}_{18}$  column (5  $\mu\text{m}$ ,  $4.6 \times 250$  mm; Agilent), attached to a KrudKatcher disposable precolumn (0.5  $\mu\text{m}$ ) filter (Phenomenex), and eluted using a gradient mobile phase of (A) 0.5% acetic acid and

(B) 100% methanol as follows: 95% A from 0 to 7 min, 95% to 70% A from 7 to 9 min, and then 70% to 95% A from 9 to 11 min with a flow rate of 0.85 mL/min. Samples were analyzed in the positive ionization mode using selected reaction monitoring (SRM) for the transitions  $m/z$  196 $\rightarrow$ 152 and 201 $\rightarrow$ 157 (26). Adduct values were corrected to take into account any contribution from the unlabeled fraction of the [ $^{14}\text{C}$ ]EO dose administered (16.7% or 91.7% at the two highest concentrations). For each sample, using the [ $^{14}\text{C}$ ]N7-HEG value determined by AMS, the number of unlabeled adducts formed by [ $^{14}\text{C}$ ]EO was calculated and then subtracted from the N7-HEG level measured by LC-MS/MS.

**HPLC isolation of [ $^{14}\text{C}$ ]N7-HEG adducts.** The remaining half of the filtrate from the neutral thermal hydrolysis was subjected to HPLC to isolate the [ $^{14}\text{C}$ ]N7-HEG peak of interest. This was performed on a Jasco instrument, comprising intelligent HPLC pumps (PY-1580), a dynamic mixer (HG-1580-32), and an intelligent sampler (AS-1555). Samples were separated using the same column type, flow rate, and gradient mobile phase used for LC-MS/MS analysis described above. UV absorbance was monitored using a multiwave detector at 254 nm. At least one blank run was performed between samples to prevent cross-contamination. Typically, fractions were collected at 15-s intervals for the run duration and then samples expected to contain [ $^{14}\text{C}$ ]N7-HEG were processed for AMS analysis (27).

**AMS analysis.** AMS analysis was carried out at the Lawrence Livermore National Laboratory according to standard protocols (28, 29). Each HPLC fraction was supplemented with 1  $\mu\text{L}$  tributyrin, providing 615  $\mu\text{g}$  carbon. Graphite samples were analyzed for radiocarbon content up to seven times or until measurement variation was within  $\pm 5\%$ . Results were converted from Fraction Modern into attomoles of  $^{14}\text{C}$  per fraction and the mean background level of  $^{14}\text{C}$ , measured in fractions collected from a blank HPLC run, was subtracted from each fraction. For each run, where individual values were above the limit of detection ( $\sim 1$  attomole  $^{14}\text{C}$ /fraction), the  $^{14}\text{C}$  content in fractions corresponding to the [ $^{14}\text{C}$ ]N7-HEG peak was summed and converted into an adduct level/ $10^{12}$  nucleotides.

**Detection of N7-HEG adducts in human colon cells.** Human colon adenocarcinoma HCA-7 cells obtained from the European Collection of Cell Cultures were maintained in DMEM supplemented with 10% FCS (Life Technologies) at  $37^\circ\text{C}$  in 5%  $\text{CO}_2$ . Cells were treated with  $\text{H}_2\text{O}_2$  (50 and 100  $\mu\text{mol}/\text{L}$ ) or vehicle (water) for 4 or 24 h. In a separate study, cells were incubated with ACC (1 mmol/L) or solvent (water) and added fresh each day after replacing the medium for a period of 7 d. Adherent cells were trypsinized and washed by centrifugation in PBS, and DNA was extracted immediately using a DNeasy kit (Qiagen). N7-HEG adducts were quantified by LC-MS/MS.

**Western blotting.** Whole-cell extracts were harvested in SDS/sample buffer [40% glycerol, 0.24 mol/L Tris (pH 6.8), 8% SDS, 20% 2-mercaptoethanol], and protein concentrations were measured by the Bradford Assay (Bio-Rad). The Protein 3 Bio-Rad Western blotting system was used with 100  $\mu\text{g}$  protein on a 10% gel. Human CYP2E1 Supersomes (BD Gentest) were used as a positive control. Membranes were probed with anti-human CYP2E1 IgG (30). The secondary antibody was anti-rabbit (Santa Cruz Biotechnology) conjugated to horseradish peroxidase.

**LC-MS/MS analysis of ACC.** Extracts of HCA-7 cells and rat liver homogenates were prepared based on a published method (31). Typically, 200 mg tissue or  $1 \times 10^6$  cells were homogenized in 100  $\mu\text{L}$  of acetone/methanol (1:4). After incubation (15 min,  $37^\circ\text{C}$ ), the supernatant was concentrated to dryness and reconstituted in mobile phase (100  $\mu\text{L}$ ). Chromatographic separations were carried out on a Waters Atlantis  $\text{C}_{18}$  3  $\mu\text{m}$  column (2.1  $\times$  150 mm) with isocratic elution using 1.8 mmol/L nonafluoropentanoic acid in water/methanol (90:10) at a flow rate of 0.19 mL/min. The column was coupled to a Micromass Quattro Ultima mass spectrometer (Waters) equipped with an electrospray interface operated in positive ion mode. ACC was detected using SRM for the transition  $m/z$  102 $\rightarrow$ 56, which results from loss of the  $-\text{CHO}_2$  moiety from the protonated molecular ion.

**Linear regression and statistical analysis.** To examine the dose-response relationship for [ $^{14}\text{C}$ ]N7-HEG adduct formation, all data were square root transformed to give a distribution closer to normality. Linear regression was then performed using the R function for modeling apparent

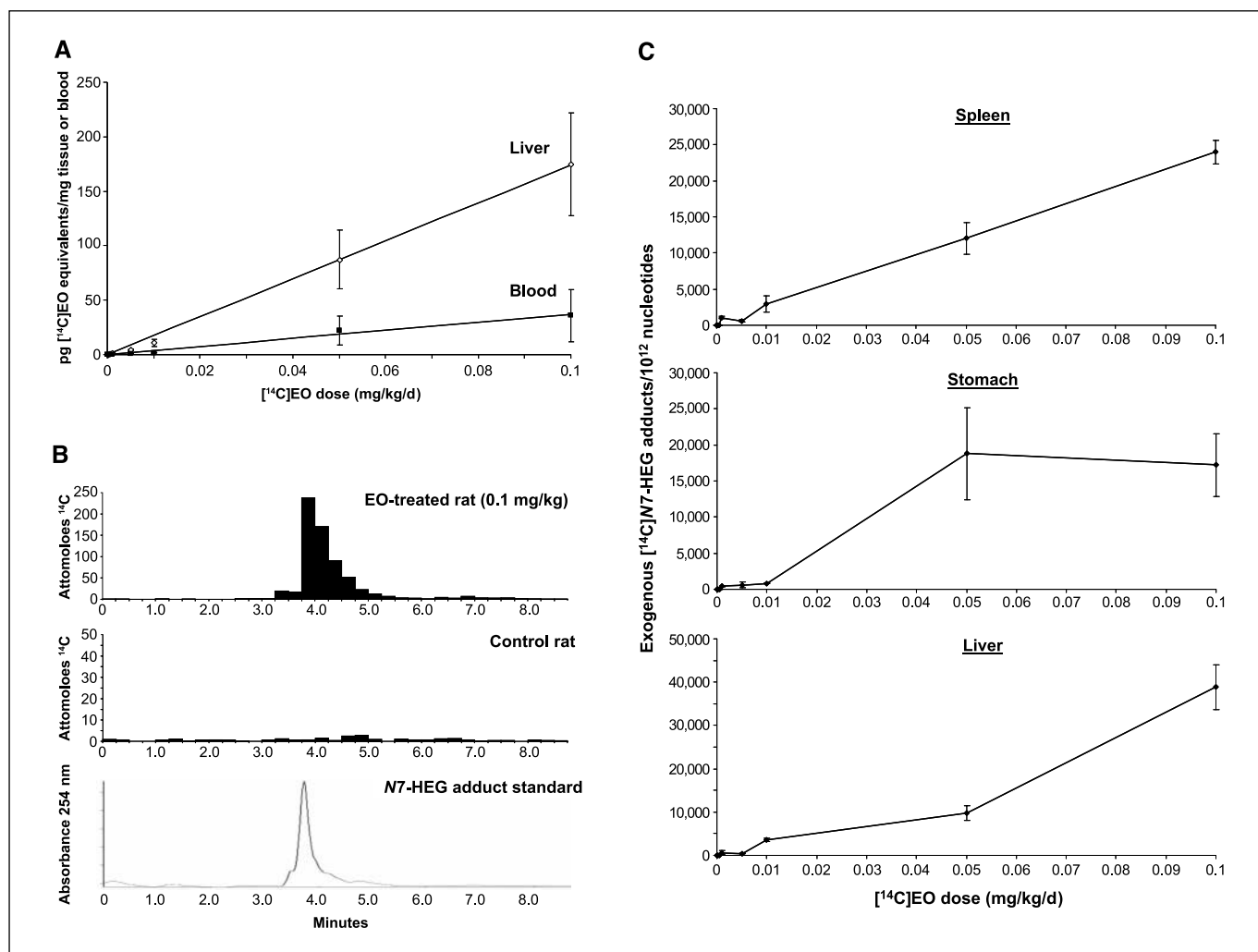


**Figure 1.** A, concentration of  $[^{14}\text{C}]$ EO equivalents in blood and liver tissue from rats treated with  $[^{14}\text{C}]$ EO (0–0.1 mg/kg). Samples were measured by LSC. Points, mean of four animals per dose; bars, SD. B, HPLC-AMS analysis of depurinated rat spleen DNA. Panels correspond to reconstructed chromatograms of filtrate collected after depurination of DNA (50  $\mu\text{g}$ ) from a rat administered  $[^{14}\text{C}]$ EO (0.1 mg/kg) and a control rat. Fractions were collected at 15-s intervals and the entire run (35 fractions) was analyzed by AMS. Also shown is a typical UV-HPLC chromatogram of an authentic N7-HEG standard (25 pmol), routinely analyzed to monitor retention time. C, relationship between  $[^{14}\text{C}]$ EO dose and level of exogenous  $[^{14}\text{C}]$ N7-HEG formed in rat tissues. Points, mean of three animals per treatment group; bars, SE.

thresholds by a hockey stick model (kindly provided by Prof. Werner Lutz, University of Würzburg, Würzburg, Germany).<sup>4</sup> Having identified the best fitting model, the first concentration of  $[^{14}\text{C}]$ EO to yield a significant increase ( $P < 0.05$ ) in adduct levels over background was determined using an approach devised and kindly provided by the BioStatistics Department at Covance Laboratories. The control (group 0) was compared with the lowest concentration of 0.0001 mg/kg (group 1) using a one-sided two-sample  $t$  test. Groups 0 and 1 combined were then compared with the 0.0005 mg/kg dose (group 2) using the same test. Subsequently, each concentration was compared with the previous three combined, after first testing whether these were similar (equality of the means) using a one-way ANOVA. The first significant value was defined as the concentration that produced a statistically significant ( $P < 0.05$ ) difference from the preceding concentrations, with all higher concentrations having the same or greater response. All other DNA adduct data were analyzed by the Student's  $t$  test using Microsoft Excel.

<sup>4</sup> W. Lutz et al., submitted for publication.

## Results and Discussion

**$[^{14}\text{C}]$ EO blood and tissue concentrations.** Daily administration of  $[^{14}\text{C}]$ EO to rats by i.p. injection for 3 days over a dose range spanning 3 orders of magnitude resulted in a linear, dose-dependent increase in both blood and liver concentrations of  $[^{14}\text{C}]$ EO equivalents (Fig. 1A). Tissue levels were higher than blood, typically by a factor of  $\sim 5$ , with maximum concentrations of  $\sim 175$  pg/mg achieved following the 0.1 mg/kg dose. Blood levels ranged from  $\sim 0.1$  to 36 pg/mg  $[^{14}\text{C}]$ EO equivalents between the 0.0005 and 0.1 mg/kg doses. Despite environmental monitoring and information on external exposures, there is a paucity of data on internal exposure to EO in terms of blood or tissue concentrations in humans. A physiologic-based pharmacokinetic model developed by Fennel and colleagues (32) and validated using data from workers in a hospital sterilizing unit (33) describes blood concentrations up to a maximum of  $\sim 105$   $\mu\text{g}/\text{L}$  ( $\sim 105$  pg/mg) for EO air levels reaching  $\sim 12.5$  ppm. Moreover, exposures of  $\sim 1$  ppm, the 8-hour time weighted average permissible exposure

**Table 1.** Levels of endogenously and exogenously derived DNA adducts in tissues of [<sup>14</sup>C]EO-treated rats measured by LC-MS/MS and AMS, respectively

[ <sup>14</sup> C]EO dose (mg/kg)	Levels of exogenous and endogenous DNA adducts per 10 <sup>10</sup> nucleotides (mean ± SE)					
	Liver		Spleen		Stomach	
	[ <sup>14</sup> C]N7-HEG	N7-HEG	[ <sup>14</sup> C]N7-HEG	N7-HEG	[ <sup>14</sup> C]N7-HEG	N7-HEG
Control	0.16 ± 0.09	233 ± 42	0.08 ± 0.05	242 ± 40	0.00	373 ± 30
0.0001	0.25 ± 0.13	312 ± 12	0.22 ± 0.05	349 ± 202	0.00	363 ± 58
0.0005	0.55 ± 0.28	296 ± 35	0.22 ± 0.10	376 ± 167	0.27 ± 0.07*	298 ± 72
0.001	6.49 ± 5.09	743 ± 234	10.68 ± 1.26*	396 ± 265	4.19 ± 0.73	283 ± 34
0.005	4.45 ± 1.04*	763 ± 218	6.12 ± 1.38	605 ± 161	6.17 ± 3.60	346 ± 37
0.01	36.16 ± 3.92	487 ± 133	29.31 ± 10.91	324 ± 18	8.43 ± 0.30	287 ± 44
0.05	97.60 ± 16.73	578 ± 7	120.23 ± 22.14	910 ± 176	188.00 ± 64.02	340 ± 204
0.1	388.57 ± 51.54	1,532 ± 425	239.67 ± 16.59	1,461 ± 360	172.15 ± 43.61	418 ± 81

NOTE: Values are the mean ± SE for three rats per group. For the [<sup>14</sup>C]N7-HEG adducts only, formed by direct reaction of [<sup>14</sup>C]EO with DNA, the first level of damage identified as being significantly higher than the background radiocarbon in control animals is designated by \* ( $P < 0.05$ ).

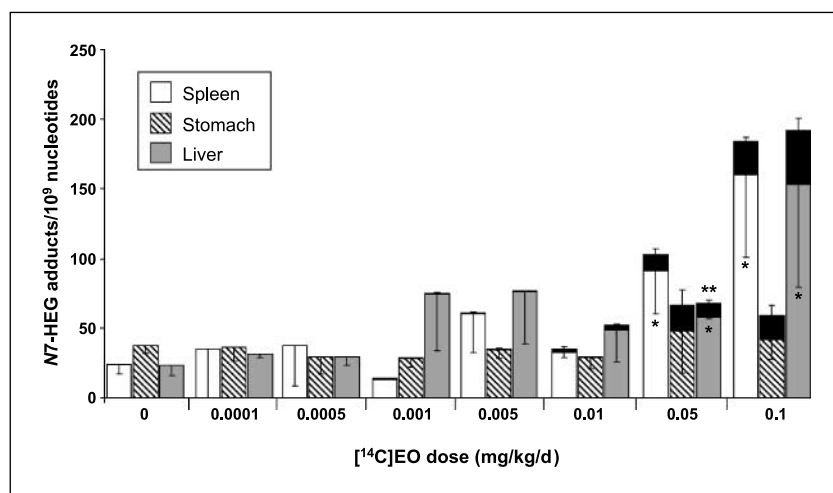
limit for airborne EO in the United States, were associated with blood concentrations of <20 µg/L (~20 pg/mg). Importantly, this indicates that the blood concentrations attained in rats encompass the range to which humans are subjected, with doses <0.05 mg/kg approximating to exposures of <1 ppm.

**Dose-response relationship for [<sup>14</sup>C]N7-HEG and N7-HEG adducts.** To define the dose-response relationship for adducts formed as a direct consequence of exogenous EO exposure, the levels of [<sup>14</sup>C]N7-HEG in rat tissues were quantified by HPLC-AMS. A HPLC separation step was incorporated before AMS analysis, rather than simply measuring radiocarbon in the total filtrate produced from thermal depurination of DNA, to specifically isolate the adduct of interest and remove any interfering lesions such as N3-2-hydroxyethyladenine (N3-HEA), which would also be liberated under these conditions (11). Using the HPLC system employed N3-HEA elutes before and is completely resolved from the N7-HEG adduct (data not shown); therefore, it does not contribute to the measured <sup>14</sup>C level. AMS analysis of an entire HPLC run of the thermal depurination products from spleen DNA of a treated rat (0.1 mg/kg) revealed a single discrete peak of radioactivity eluting

around 3.5 to 4.5 minutes (Fig. 1B, *top trace*), which corresponds in retention time to the authentic N7-HEG standard (Fig. 1B, *bottom trace*). As expected, no peaks due to excess radiocarbon were evident in the reconstructed chromatogram from a control rat that did not receive [<sup>14</sup>C]EO (*middle trace*).

The amount of [<sup>14</sup>C]N7-HEG in each spleen, stomach, and liver DNA sample was determined by summation of the <sup>14</sup>C content in individual HPLC fractions comprising the adduct peak (Table 1). Importantly, exogenous adduct formation was dose dependent in all tissues (Fig. 1C) and modeling of the data revealed that the response was significant for a linear relationship ( $P < 0.05$ ) in all three tissues, as opposed to the alternative hypothesis of a hockey stick model, which did not explain a significantly greater proportion of the variation. However, it should be appreciated that because this study was not specifically designed to test for linearity and some of the adduct levels induced at lower [<sup>14</sup>C]EO concentrations are below the limit of quantitation (~20–50 adducts/10<sup>12</sup> nucleotides), they may not be sufficiently accurate to allow unambiguous establishment of a linear dose response. Confirmation, or indeed rejection, of the prediction presented here

**Figure 2.** Contribution of endogenously and exogenously derived N7-HEG to the total adduct level in tissues of [<sup>14</sup>C]EO-treated rats. Endogenous adducts were determined by LC-MS/MS. Exogenous <sup>14</sup>C-labeled adducts were quantified by AMS and are shown as black bars on top of bars representing endogenous adduct levels. Columns, mean of three animals per group; bars, SD. \*,  $P < 0.05$ , the level of endogenous N7-HEG in tissues of [<sup>14</sup>C]EO-treated rats is significantly higher than the corresponding background level in control animals; \*\*,  $P < 0.05$ , the total level of adducts (endogenous plus exogenous) is significantly higher than the level of endogenous adducts alone in a particular tissue.



may be achieved by including additional low doses at 0.00025, 0.00075, 0.0025, and 0.0075 mg/kg, which are spaced well below that of a multiple of  $\sqrt{10}$ .

At the lowest dose of 0.0001 mg/kg, no adducts were observed in stomach DNA, indicating they were either not formed or perhaps more likely were present at levels below the limit of detection (which ranged from 4 to 10 adducts/ $10^{12}$  nucleotides). Statistical analysis showed that the first significant ( $P < 0.05$ ) increases in  $^{14}\text{C}$ -labeled exogenous adducts above background levels of radiocarbon detected in control rats occurred at 0.005, 0.001, and 0.0005 mg/kg for the liver, spleen, and stomach, respectively; the fact that these values do not equate to the lowest dose can probably be attributed to the relatively large interindividual variation. The biological risks associated with these adducts can only be evaluated if the data are viewed in a wider context, taking into account background levels of this lesion.

Using our established LC-MS/MS assay for *N7*-HEG, it was possible to accurately quantify the background (unlabeled) adduct level in rat tissues, distinct from those formed as a consequence of [ $^{14}\text{C}$ ]EO reacting with DNA. It is clearly evident from Fig. 2, which displays the relative proportion of endogenously derived *N7*-HEG and exogenous [ $^{14}\text{C}$ ]N7-HEG in tissues, that exogenous adducts comprise a relatively small fraction of the total damage, especially at doses  $\leq 0.005$  mg/kg, where [ $^{14}\text{C}$ ]N7-HEG accounts for  $<2\%$  of the total adducts detected and can be considered negligible. The maximum proportion of exogenous adducts (29%) occurs in the stomach after dosing with 0.1 mg/kg [ $^{14}\text{C}$ ]EO. However, given the inherent variation in endogenous adduct levels among rats, it is important to recognize that the increase in adducts caused by direct binding of [ $^{14}\text{C}$ ]EO to DNA is not significant at any dose, with the single exception of hepatic tissue of rats that received 0.05 mg/kg ( $P < 0.05$ ). The important implications of this finding are that exogenous *N7*-HEG formation may not pose any additional risk over and above that presented by the ubiquitous background damage, a suggestion that is reinforced when the results are translated to humans. At doses of 0.05 mg/kg, which yields blood concentrations of [ $^{14}\text{C}$ ]EO equivalents in the order of 22 pg/mg, making it relevant to human occupational exposures (33), the extent of [ $^{14}\text{C}$ ]N7-HEG formation in rat tissues was around 10 to 20 adducts/ $10^9$  nucleotides; this is 5- to 100-fold lower than the endogenous level of these adducts reported in WBCs isolated from unexposed humans (16–18).

Interestingly, EO treatment did affect the total numbers of *N7*-HEG lesions formed through an indirect mechanism, a phenomenon that has never before been observed. The background abundance of endogenous *N7*-HEG in control untreated animals was  $24.2 \pm 6.9$ ,  $37.3 \pm 5.1$ , and  $23.3 \pm 7.3$  adducts/ $10^9$  nucleotides (mean  $\pm$  SD) in spleen, stomach, and liver, respectively, which agrees with previous values obtained in rats (Fig. 2; ref. 26). At doses up to and including 0.01 mg/kg, [ $^{14}\text{C}$ ]EO administration had no significant effect on the presence of endogenous lesions. However, at the two highest doses, endogenous (unlabeled) *N7*-HEG formation in the spleen and liver was significantly higher than levels in control animals, reaching  $91.0 \pm 30.5$  and  $160.2 \pm 59.2$  adducts/ $10^9$  nucleotides in the spleen and  $57.8 \pm 1.3$  and  $153.2 \pm 73.6$  in the liver at 0.05 and 0.1 mg/kg [ $^{14}\text{C}$ ]EO, respectively. This suggests that exposure to EO induces physiologic pathways responsible for ethylene generation *in vivo* and, as a consequence, indirectly increases *N7*-HEG adduct levels.

**Endogenous formation of *N7*-HEG in cells subjected to oxidative stress.** The sources of endogenous ethylene production

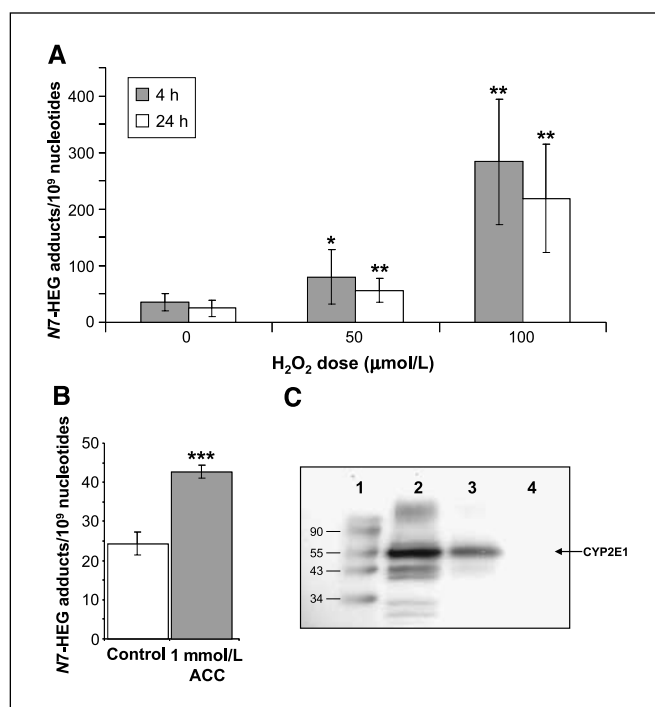


**Figure 3.** A, levels of *N7*-HEG induced in HCA-7 cells following treatment with  $\text{H}_2\text{O}_2$  (0–100  $\mu\text{mol/L}$ ) for 4 or 24 h. Incubations were conducted on three separate occasions and adduct levels were quantified in at least two replicates per experiment ( $n = 6$ –8) by LC-MS/MS, apart from one instance where only one sample was analyzed for the 100  $\mu\text{mol/L}$  dose at 4 h (giving  $n = 5$ ). \*,  $P < 0.05$ ; \*\*,  $P < 0.005$ , the level of *N7*-HEG in  $\text{H}_2\text{O}_2$ -treated cells is significantly higher than levels in control cells. B, *N7*-HEG levels in cells cultured in the presence or absence of ACC (1 mmol/L) for 7 d. Values are the mean of three independent experiments, with up to six replicates conducted per experiment. \*\*\*,  $P < 0.0005$ , the adduct level is significantly higher than in control cells. C, Western blotting reveals the presence of CYP2E1 in human HCA-7 cells. Lane 1, molecular weight standard; lane 2, recombinant human CYP2E1 Supersomes (0.02 pmol cytochrome P450 content); lane 3, cell extract (100  $\mu\text{g}$  protein); lane 4, buffer only.

in mammalian systems have not been directly determined. Pathways frequently cited to account for the presence of *N7*-HEG in animals and humans include oxidation of methionine, lipid peroxidation, and the metabolizing activity of intestinal bacteria; however, the underlying mechanisms have not been elucidated. Methionine is undeniably a precursor of ethylene in plant tissues, where the gas acts as an important hormone to regulate growth, development, and senescence (19). In model *in vitro* systems, ethylene is produced from methionine in a process mediated by  $\text{H}_2\text{O}_2$  generated in a reaction between cuprous ions, hydrogen ions, and oxygen. Furthermore, tracer studies with [ $^{14}\text{C}$ ]methionine revealed that carbons 3 and 4 of the amino acid were converted to ethylene (34). Evidence for the role of lipid peroxidation in ethylene and EO production is less defined but stems from observations that the 2-hydroxyethylvaline content in hemoglobin is higher in mice fed unsaturated lipids compared with animals on a standard diet (20). In addition, ethylene can be generated from peroxidized linolenate in model systems containing  $\text{Cu}^{2+}$ , oxygen, and ascorbic acid (19) and in cell-free apple extracts in the presence of oxygen and ascorbic acid (35). Crucially, however, when U- $^{14}\text{C}$ -labeled linolenate was used as a substrate in similar model systems with cauliflower, apple, or tomato slices, the  $^{14}\text{C}$  label was not incorporated into ethylene, showing that linolenic acid itself does not supply the two-carbon fragment of ethylene (36).

Although a mechanism through which EO exposure might enhance cellular levels of oxidative stress has not yet been defined, evidence supports the possibility. Repeated exposure to EO elevates lipid peroxidation in the liver of rats, an effect that has been attributed to glutathione depletion (37). Interestingly, administration of ethylene glycol, a metabolite of EO produced by enzymatic and spontaneous hydrolysis (32), also promotes lipid peroxidation *in vivo* (38). Moreover, ethylene glycol free radical formation has been shown to occur in a rat model of acute poisoning and it has been suggested that lipid hydroperoxide-derived radicals are also formed as a consequence of hydrogen abstraction, mediated by peroxy radicals produced from the reaction of 1,2-dihydroxyethyl radicals with molecular oxygen (39). These considerations prompted us to investigate whether increased oxidative stress might indirectly account for the elevated levels of endogenous *N7*-HEG detected in rat spleen and liver.

When human HCA-7 colon cells were incubated in the presence of  $H_2O_2$  (50 and 100  $\mu\text{mol/L}$ ) as a source of reactive oxygen species (ROS), there was a significant dose-related elevation in *N7*-HEG quantified in the extracted DNA compared with control cells (Fig. 3A). This effect was observed 4 hours after treatment commenced, when mean adduct levels were  $\sim 2$ - and 8-fold higher than the background damage for 50 and 100  $\mu\text{mol/L}$   $H_2O_2$ , respectively, and was still visible at 24 hours, although to a slightly lesser extent. This is the first direct evidence that exposure to ROS, in the form of  $H_2O_2$ , can stimulate *N7*-HEG formation, presumably as a consequence of EO production.

**ACC as a precursor to EO in rat tissues and human cells.** The mechanism of ethylene biosynthesis in plants is relatively well established and involves ACC as the immediate precursor. ACC is liberated from methionine via *S*-adenosylmethionine in a reaction that is catalyzed by ACC synthase in plants (40). It then undergoes ACC oxidase-mediated two-electron oxidation in the presence of dioxygen and a reductant to yield ethylene,  $CO_2$ , and HCN. This second reaction is inhibited by free radical scavengers (41) and

can also occur nonenzymatically in the presence of pyridoxal phosphate,  $H_2O_2$ , and manganese or when a  $Cu(II)$ -ACC complex is incubated with  $H_2O_2$  alone (42, 43). Of particular relevance to the current study is the fact that oxidation of linoleic acid by lipoxygenase in the presence of ACC generates ethylene (44). The mechanism is believed to involve generation of linoleic hydroperoxide, which is cleaved reductively to an alkoxy radical that reacts with ACC via hydride abstraction, affording an amine radical cation intermediate (45). From here, the precise sequence of events leading to the release of ethylene is still under investigation. We hypothesized that an analogous mechanism, depicted in Fig. 4, occurs in mammalian cells, in which fatty acid peroxidation induces ethylene production by supplying the alkoxy radical necessary for activation of ACC. Hence any increase in intracellular ROS or the substrates for oxidation, ACC or fatty acids, may result in higher background *N7*-HEG levels. This theory explains how EO exposure causes increased endogenous *N7*-HEG formation in rat tissues and why administration of unsaturated lipids to mice has previously been shown to cause elevated levels of 2-hydroxyethylvaline adducts in hemoglobin (20), although lipids are not a direct ethylene precursor. This premise was supported by the illustration that treatment of HCA-7 cells with 1  $\text{mmol/L}$  ACC for a week significantly increased endogenous *N7*-HEG formation from  $24 \pm 2.9$  to  $43 \pm 1.6$  adducts/ $10^9$  nucleotides ( $P < 0.0005$ ; Fig. 3B). Furthermore, the occurrence of CYP2E1 protein, the enzyme required for metabolic conversion of ethylene to EO in humans, was shown in HCA-7 cells by Western blotting, which revealed a band at 55 kDa (Fig. 3C, lane 3), consistent with the expected molecular weight and the baculovirus-expressed recombinant human CYP2E1 standard in Fig. 3C (lane 2).

The outstanding question remaining was whether the vital component of this system, ACC, occurs naturally in mammalian cells. To our knowledge, this has never previously been reported; therefore, using an ion exchange LC-MS/MS method adapted from a published assay for ACC in plant tissue (46), we analyzed extracts

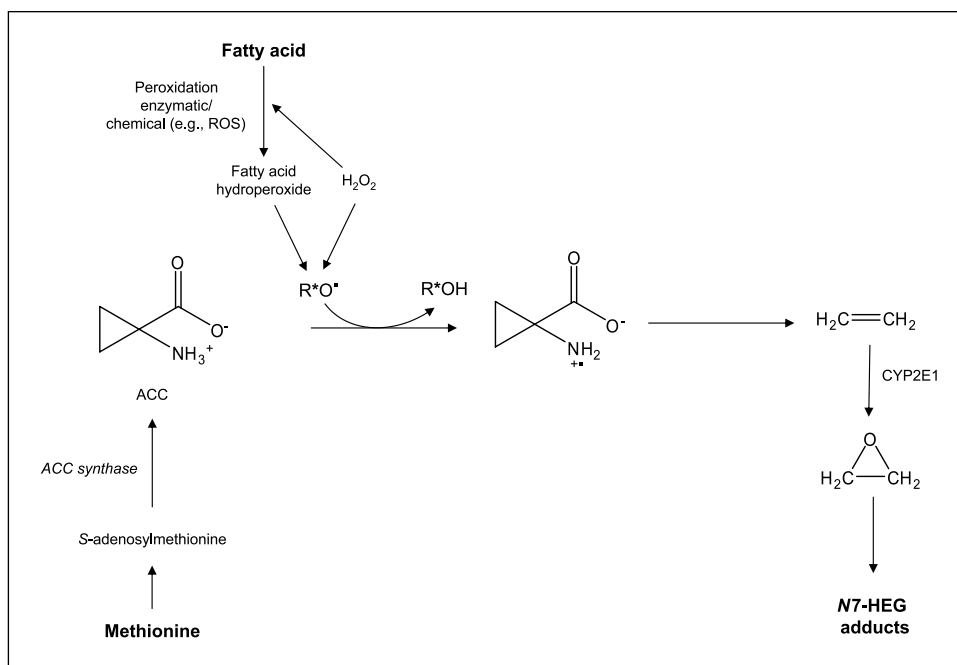
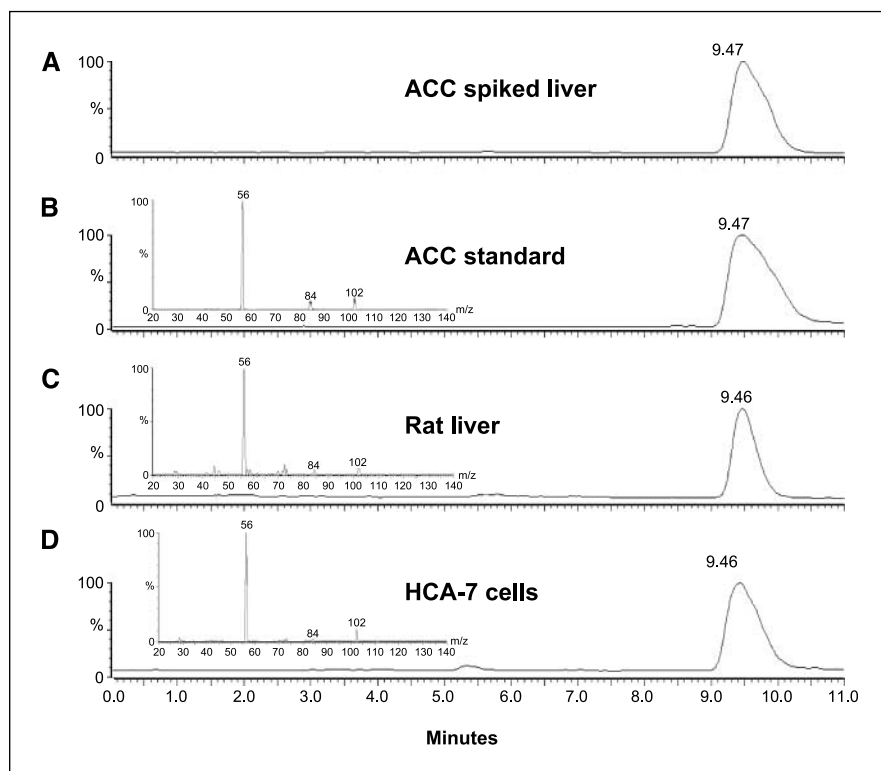


Figure 4. Proposed pathway of endogenous *N7*-HEG formation *in vivo*.



**Figure 5.** Detection of ACC in human HCA-7 cells and liver tissue from an untreated control rat by ion exchange LC-MS/MS with SRM for the transition  $m/z$  102→56. Traces correspond to extracts (10  $\mu$ L) of (A) rat liver spiked with ACC, (C) rat liver, (D) HCA-7 cells, and (B) an authentic ACC standard (10 pmol). The product ion spectra (*inset*) were obtained by selecting  $m/z$  102 as the parent ion and scanning from  $m/z$  40 to 105.

of rat liver and HCA-7 cells for the presence of endogenous ACC (Fig. 5). Peaks with the same retention time as an authentic ACC standard were detected in both tissue and cells using SRM for the characteristic transition  $m/z$  102→56, which corresponds to loss of formic acid from the protonated molecular ion. For comparison and to assess any matrix effects, a separate liver sample spiked with ACC was also analyzed and gave identical results. Product ion spectra obtained for each sample (see *insets*, Fig. 5) by selecting  $m/z$  102 as the parent ion and scanning from  $m/z$  40 to 105 provided further confirmation that the peaks were due to ACC, as all afforded similar spectra.

In summary, by using a dual-isotope approach combining HPLC-AMS with LC-MS/MS analysis, we have provided evidence supporting a linear dose-response relationship for the major EO DNA adduct after exposure to low occupationally relevant doses. More importantly, we have proven that the extent of damage arising through this route is insignificant compared with the background level of *N7*-HEG naturally present. As a direct consequence of the analytic strategy used, it was possible to detect a specific increase in endogenously derived *N7*-HEG caused by EO exposure at the higher doses and we propose a novel mechanism of adduct formation to account for this effect, involving oxidative stress. *N7*-HEG is only one of a variety of DNA adducts induced by oxidative stress, including many that are promutagenic. Such lesions are very likely to contribute to the background mutations that are involved in carcinogenesis. These findings therefore have implications for human risk assessments and suggest that *N7*-HEG adduct levels may have potential as a biomarker of cellular oxidative stress.

The default position for many regulators when assessing the risk from genotoxic carcinogens is to assume that there is no threshold

in the dose-response relationship and that even very low doses cause an incremental risk. However, as shown here, if the compound is produced endogenously, low doses of exogenous exposure may be overwhelmed by the background levels, leading to no detectable statistically significant increase in risk due to the external exposure. To assess the importance of this phenomenon to the regulation of EO exposures, it will firstly be essential to determine the variation of *N7*-HEG levels in “unexposed” control human populations and to identify the modulating factors for this background. Similar studies on populations exposed to low levels of exogenous EO would then enable determination of whether a practical threshold exists and if a dose range could be established for this. The presence of background levels of EO, and possibly induced cancer risk, must be borne in mind when interpreting past and future epidemiologic studies.

## Disclosure of Potential Conflicts of Interest

No potential conflicts of interest were disclosed.

## Acknowledgments

Received 11/5/08; revised 1/12/09; accepted 1/14/09; published OnlineFirst 3/10/09.

**Grant support:** American Chemistry Council grant MTH0311-02 and Cancer Research UK grant C325/A6691. AMS analysis was performed at the Research Resource for Biomedical AMS Laboratory, operated at the Lawrence Livermore National Laboratory, and supported by NIH, National Center for Research Resources, Biomedical Technology Program grant P41RR13461.

The costs of publication of this article were defrayed in part by the payment of page charges. This article must therefore be hereby marked *advertisement* in accordance with 18 U.S.C. Section 1734 solely to indicate this fact.

We thank Manijeh Maleki-Dizaji for technical assistance, Kurt Haack for graphitization of AMS samples, Dr. Ken Turteltaub for helpful comments, and Dr. Jerome Lasker (Hackensack University Medical Center) for kindly providing the anti-human CYP2E1 IgG antibody.

## References

1. Thier R, Bolt HM. Carcinogenicity and genotoxicity of ethylene oxide: new aspects and recent advances. *Crit Rev Toxicol* 2000;30:595-608.
2. NTP. 10th Report on carcinogens. Research Triangle Park (NC): U.S. Department of Health and Human Services, Public Health Service, National Institutes of Health, National Toxicology Program; 2002.
3. Hogstedt C, Malmqvist N, Wadman B. Leukaemia in workers exposed to ethylene oxide. *JAMA* 1979;241:1132-3.
4. Hogstedt C, Rohlen O, Berndtsson B, Axelson O, Ehrenberg L. A cohort study of mortality and cancer incidence in ethylene oxide production workers. *Br J Ind Med* 1979;36:276-80.
5. Hogstedt C, Aringer L, Gustavsson A. Epidemiologic support for ethylene-oxide as a cancer-causing agent. *JAMA* 1986;255:1575-8.
6. Teta MJ, Sielken RL, Valdez-Flores C. Ethylene oxide cancer risk assessment based on epidemiological data: application of revised regulatory guidelines. *Risk Analysis* 1999;19:1135-55.
7. Coggon D, Harris EC, Poole J, Palmer KT. Mortality of British workers exposed to ethylene oxide: extended follow up of a British cohort. *Occup Environ Med* 2004;61:358-62.
8. Steenland K, Stayner J, Deddens J. Mortality analyses in a cohort of 18235 ethylene oxide exposed workers: follow up extended from 1987 to 1998. *Occup Environ Med* 2004;61:2-7.
9. Hogstedt B, Gullberg B, Hedner K, et al. Chromosome aberrations and micronuclei in bone marrow cells and peripheral blood lymphocytes in humans exposed to ethylene oxide. *Hereditas* 1983;98:105-13.
10. IARC. Some industrial chemicals: ethylene oxide. In: *International Agency for Research on Cancer. IARC monographs on the evaluation of carcinogenic risks to humans*, vol. 60. Lyon (France): IARC; 1994. p. 73-159.
11. Walker VE, Fennell TR, Upton PB, et al. Molecular dosimetry of ethylene oxide: formation and persistence of N7-(2-hydroxyethyl)guanine in DNA following repeated exposure of rats and mice. *Cancer Res* 1992;52:4328-34.
12. Li F, Segal A, Solomon JJ. *In vitro* reaction of ethylene oxide with DNA and characterization of DNA adducts. *Chem Biol Interact* 1992;83:35-54.
13. Takeshita M, Chang C-H, Johnson F, Will S, Grollman AP. Oligonucleotides containing synthetic abasic sites: model substrates for DNA-polymerases and apurinic apyrimidinic endonucleases. *J Biol Chem* 1987;262:10171-9.
14. Loeb LA, Preston BD. Mutagenesis by apurinic apyrimidinic sites. *Ann Rev Gen* 1986;20:201-30.
15. IARC. Some industrial chemicals: ethylene oxide. In: *International Agency for Research on Cancer. IARC monographs on the evaluation of carcinogenic risks to humans*, vol. 60. Lyon (France): IARC; 1994. p. 45-71.
16. Wu KY, Scheller N, Ranasinghe A, et al. A gas chromatography/electron capture/negative chemical ionization high-resolution mass spectrometry method for analysis of endogenous and exogenous N7-(2-hydroxyethyl)guanine in rodents and its potential for human biological monitoring. *Chem Res Toxicol* 1999;18:722-9.
17. Zhao C, Hemminki K. The *in vivo* levels of DNA alkylation products in human lymphocytes are not age dependent: an assay of 7-methyl- and 7-(2-hydroxyethyl)-guanine DNA adducts. *Carcinogenesis* 2002;23:307-10.
18. Yong LC, Schulte PA, Kao CY, et al. DNA adducts in granulocytes of hospital workers exposed to ethylene oxide. *Am J Ind Med* 2007;50:293-302.
19. Liberman M, Mapson LW. Genesis and biogenesis of ethylene. *Nature* 1964;204:343-5.
20. Törnqvist M, Gustafsson B, Kautiainen A, Harms-Ringdahl M, Granath F, Ehrenberg L. Unsaturated lipids and intestinal bacteria as sources of endogenous production of ethene and ethylene oxide. *Carcinogenesis* 1989;10:39-41.
21. Beauchamp C, Fridovich I. A mechanism for the production of ethylene from methional. The generation of the hydroxyl radical by xanthine oxidase. *J Biol Chem* 1970;245:4641-6.
22. Henderson L, Albertini S, Aardema M. Thresholds in genotoxicity responses. *Mut Res* 2000;464:123-8.
23. Doak SH, Jenkins GJS, Johnson GE, Quick E, Parry EM, Parry JM. Mechanistic influences for mutation induction curves after exposure to DNA-reactive carcinogens. *Cancer Res* 2007;67:3904-11.
24. Swenberg JA, Fryar-Tita E, Jeong YC, et al. Biomarkers in toxicology and risk assessment: informing critical dose-response relationships. *Chem Res Toxicol* 2008;21:253-65.
25. Brown K, Tompkins EM, White INH. Applications of accelerator mass spectrometry for pharmacological and toxicological research. *Mass Spectrom Rev* 2006;25:127-45.
26. Marsden DA, Jones DJL, Lamb JH, Tompkins E, Farmer PB, Brown K. Determination of endogenous and exogenously derived N7-(2-hydroxyethyl)guanine adducts in ethylene oxide treated rats. *Chem Res Toxicol* 2007;20:290-9.
27. Brown K, Dingley KH, Turteltaub KW. Accelerator mass spectrometry for biomedical research. *Methods Enzymol* 2005;402:423-43.
28. Ognibene TJ, Bench G, Brown TA, Peaslee GF, Vogel JS. A new accelerator mass spectrometry system for <sup>14</sup>C-quantification of biochemical samples. *Int J Mass Spectrom* 2002;218:255-64.
29. Ognibene TJ, Bench G, Vogel JS. A high-throughput method for the conversion of CO<sub>2</sub> obtained from biochemical samples to graphite in septa-sealed vials for quantification of <sup>14</sup>C via accelerator mass spectrometry. *Anal Chem* 2003;75:2192-6.
30. Carpenter SP, Lasker JM, Raucy JL. Expression, induction, and catalytic activity of the ethanol-inducible cytochrome P450 (CYP2E1) in human fetal liver and hepatocytes. *Mol Pharmacol* 1996;49:260-8.
31. Jones DJL, Lim CK, Ferry DR, Gescher A. Determination of quercetin in human plasma by HPLC with spectrophotometric or electrochemical detection. *Biomed Chromatogr* 1998;12:232-5.
32. Fennell TR, Brown CD. A physiologically based pharmacokinetic model for ethylene oxide in mouse, rat and human. *Toxicol Appl Pharmacol* 2001;173:161-75.
33. Brugnone F, Perbellini L, Faccini GB, Pasini F, Bartolucci GB, DeRosa E. Ethylene oxide exposure: biological monitoring by analysis of alveolar air and blood. *Int Arch Occup Environ Health* 1986;58:105-12.
34. Liberman M, Kunishi AT, Mapson LW, Wardale DA. Stimulation of ethylene production in apple tissue slices by methionine. *Plant Physiol* 1966;41:376-82.
35. Galliard T, Hulme AC, Rhodes MJC, Wooltorton LSC. Enzymic conversion of linolenic acid to ethylene by extracts of apple fruits. *FEBS Lett* 1968;1:283-6.
36. Mapson LW, March JF, Rhodes MJC, Wooltorton LSC. A comparative study of the ability of methionine or linolenic acid to act as precursors of ethylene in plant tissues. *Biochem J* 1970;117:473-9.
37. Katoh T, Higashi K, Inoue N, Tanaka I. Lipid peroxidation and the metabolism of glutathione in rat liver and brain following ethylene oxide inhalation. *Toxicology* 1989;58:1-9.
38. Celi I, Suzek H. Effects of subacute treatment of ethylene glycol on serum marker enzymes and erythrocyte and tissue antioxidant defense systems and lipid peroxidation in rats. *Chem Biol Interact* 2007;167:145-52.
39. Kadiiska MB, Mason RP. Ethylene glycol generates free radical metabolites in rats: an ESR *in vivo* spin trapping investigation. *Chem Res Toxicol* 2000;13:1187-91.
40. Adams DO, Yang SF. Ethylene biosynthesis: identification of 1-aminocyclopropane-1-carboxylic acid as an intermediate in the conversion of methionine to ethylene. *Proc Natl Acad Sci U S A* 1979;76:170-4.
41. Apelbaum A, Wang SY, Burgoon AC, Baker JE, Liberman M. Inhibition of the conversion of 1-aminocyclopropane-1-carboxylic acid to ethylene by structural analogs, inhibitors of electron transfer, uncouplers of oxidative phosphorylation, and free radical scavengers. *Plant Physiol* 1981;67:74-9.
42. Boller T, Herner RC, Kende H. Assay for and enzymatic formation of an ethylene precursor, 1-aminocyclopropane-1-carboxylic acid. *Planta* 1979;145:293-303.
43. Ghattas W, Gaudin C, Giorgi M, Rockenbauer A, Simaan AJ, Réglier M. ACC-oxidase like activity of a copper (II)-ACC complex in the presence of hydrogen peroxide. Detection of a reaction intermediate at low temperature. *Chem Commun* 2006;1027-9.
44. Bousquet JF, Thimann KV. Lipid peroxidation forms ethylene from 1-aminocyclopropane-1-carboxylic acid and may operate in leaf senescence. *Proc Natl Acad Sci U S A* 1984;81:1724-7.
45. Pirrung MC. Mechanism of a lipoxygenase model for ethylene biosynthesis. *Biochemistry* 1986;25:114-9.
46. Petritis K, Koukaki G, Koussissi E, Elfakir C, Dreux M, Dourtooglou V. The simultaneous determination of 1-aminocyclopropane-1-carboxylic acid and cyclopropane-1,1-dicarboxylic acid in *Lycopersicon esculentum* by high-performance liquid chromatography-electrospray tandem mass spectrometry. *Phytochem Anal* 2003;14:347-51.

# Cancer Research

The Journal of Cancer Research (1916–1930) | The American Journal of Cancer (1931–1940)

## Dose-Response Relationships for *N*-7-(2-Hydroxyethyl)Guanine Induced by Low-Dose [<sup>14</sup>C]Ethylene Oxide: Evidence for a Novel Mechanism of Endogenous Adduct Formation

Debbie A. Marsden, Donald J.L. Jones, Robert G. Britton, et al.

*Cancer Res* 2009;69:3052-3059. Published OnlineFirst March 10, 2009.

**Updated version** Access the most recent version of this article at:  
doi:[10.1158/0008-5472.CAN-08-4233](https://doi.org/10.1158/0008-5472.CAN-08-4233)

**Cited articles** This article cites 42 articles, 12 of which you can access for free at:  
<http://cancerres.aacrjournals.org/content/69/7/3052.full#ref-list-1>

**E-mail alerts** [Sign up to receive free email-alerts](#) related to this article or journal.

**Reprints and Subscriptions** To order reprints of this article or to subscribe to the journal, contact the AACR Publications Department at [pubs@aacr.org](mailto:pubs@aacr.org).

**Permissions** To request permission to re-use all or part of this article, use this link <http://cancerres.aacrjournals.org/content/69/7/3052>. Click on "Request Permissions" which will take you to the Copyright Clearance Center's (CCC) Rightslink site.